Research Paper

Journal of Chemical Research

Journal of Chemical Research
2020, Vol. 44(7-8) 367–375

DOI: 10.1177/1747519820902684
journals.sagepub.com/home/chl
SAGE

New chalcone-substituted metallophthalocyanines: Synthesis, characterization, and investigation of their properties

Ayse Aktas Kamiloglu[1], Hüseyin Karaca[2], Gonca Celik[3], Irfan Acar[4] and Halit Kantekin[3]

Abstract

The synthesis of novel metallophthalocyanines (M = Zn, Mg, and Co) derived from (*E*)-3-(3-bromophenyl)-1-(3-hydroxyphenyl)prop-2-en-1-one and (*E*)-3-(3-fluorophenyl)-1-(3-hydroxyphenyl)prop-2-en-1-one is achieved. These complexes and the synthesized novel phthalonitrile derivatives are characterized by FTIR, ^{1}H NMR, ^{13}C NMR, UV-Vis, mass spectrometry, and elemental analysis. The aggregation properties of the metallophthalocyanines ZnPc, MgPc, and CoPc are investigated in different solvents and at different concentrations in dimethyl formamide. The electrochemical behavior is also investigated. The cyclic voltammograms give one oxidation reaction for all the bromo-derived metallophthalocyanines and one reduction reaction for all the fluoro-derived metallophthalocyanines. Fe^{3+}, Cd^{2+}, Hg^{2+}, Cu^{2+}, Ni^{2+}, and Co^{2+} ions are titrated fluorometrically with the phthalocyanines. The bromo- and fluoro-substituted phthalocyanine compounds show different effects on the metal ion titrations.

Keywords

aggregation, chalcones, cyclic redox, metal-sensing, phthalocyanines

Date received: 30 July 2019; accepted: 8 January 2020

Introduction

Phthalocyanines (PCs) have been examined at an increasing rate since their discovery.[1] This macrocyclic molecule with 18 π-electrons in the conjugated system can be easily synthesized, can be derivatized from peripheral positions to tetra, and can also be derivatized from non-peripheral positions.[2–5] This allows for the formation of a rich pool of molecules and to the design of PCs that can be applied in many different applications. Because of their macrocyclic aromatic structure, simple derivatization and easy electron exchange, PCs are frequently used in areas such as catalysis,[6] organic photovoltaic devices and solar cells,[7] electrophotography,[8] Langmuir–Blodgett films,[9] photosensitizers in photodynamic therapy,[10] electrochromic displays,[11] liquid crystals,[12] and optical disks.[13]

The solubilization of PCs is necessary for their use in various applications and to improve their low solubility.[14] Two methods are applied for this purpose. The first is the choice of the central metal ion to increase the interaction with solvent molecules. The second is substitution with small moieties. The latter method is also expected to give additional properties to the PC derivative.[15,16]

Recently, the sensor and biological activities of chalcones have been studied and diverse biological activities have been found, for example, antioxidant, cytotoxic, antiviral, tyrosinase inhibitory, antimalarial, antibacterial, and anti-inflammatory.[17–19] In addition, chalcones are used as stating materials for synthesizing many compounds such as flavones, thiadiazines, isoxazoles, quinolinones, benzodiazepines, benzothiazepines, and benzofuranones.[20] Derivation of PCs with chalcones and the applications of these new compounds are quite new. With PCs derived from chalcones, applications as metal sensors,[21] catalysts,[22] photovoltaic devices, and solar cells[23] have been described. Both

[1]Artvin Vocational School, Artvin Çoruh University, Artvin, Turkey
[2]Department of Chemistry, Sakarya University, Sakarya, Turkey
[3]Department of Chemistry, Faculty of Science, Karadeniz Technical University, Trabzon, Turkey
[4]Department of Energy Systems Engineering, Faculty of Technology, Karadeniz Technical University, Trabzon, Turkey

Corresponding author:
Ayse Aktas Kamiloglu, Artvin Vocational School, Artvin Çoruh University, 08100 Artvin, Turkey.
Emails: ayse_aktas_kamiloglu@artvin.edu.tr; ayse_aktas_kamiloglu@yahoo.com

colorimetric and fluorometric techniques have been studied in metal titrations of PCs derived with chalcones.[24]

In this study, the novel phthalonitrile derivatives **3** and **4** and the novel metallophthalocyanines (MPcs; M = Zn, Mg, and Co) derived from (*E*)-3-(3-bromophenyl)-1-(3-hydroxyphenyl)prop-2-en-1-one **3a–c** and (*E*)-3-(3-fluorophenyl)-1-(3-hydroxyphenyl)prop-2-en-1-one **4a–c** have been synthesized and then characterized by Fourier-transform infrared spectroscopy (FTIR), ^{1}H NMR, ^{13}C NMR, UV-Vis, mass spectrometry, and elemental analysis. In addition, the aggregation properties of the newly synthesized chalcone-substituted PC compounds **3a–c and 4a–c** are described. The electrochemical properties of the synthesized PCs are also investigated. Fe^{3+}, Cd^{2+}, Hg^{2+}, Cu^{2+}, Ni^{2+}, and Co^{2+} ions were titrated and studied by fluorescence spectroscopy with the zinc complexes of both bromo- and fluoro-substituted PCs. Some ions selectively increase the fluorescence emissions of PCs in these titrations.

Results and discussion

Synthesis

The synthesis of zinc(II), magnesium(II), and cobalt(II) PCs with chalcones bearing halogen atoms was performed by the procedure described in Scheme 1. Chalcone compounds **1** and **2** were synthesized according to the literature[25] and were obtained as *E* isomers, as confirmed on the basis of their ^{1}H NMR spectra. Compounds **3** and **4** were obtained by nucleophilic S_NAr-type substitution of 4-nitrophthalonitrile and chalcone compounds **1** and **2** at 60°C in the presence of K_2CO_3 as the catalyst. Derivatization of MPCs with chalcone imparts solubility to MPcs and favorable characteristics for metal-sensing.[26]

The reaction yields for compounds **3** and **4** were 60% for both after column chromatography. The melting points of phthalonitrile compounds **3** and **4** were 76–79°C and 98–101°C, respectively. The melting point of compound **4,** substituted with an F atom, is higher than that of compound **3** bearing a Br atom. The fluorine atom is more electronegative than a bromine atom so the intermolecular forces present in compound **4** are higher than those of compound **3**.[27] The structures of **3** and **4** were determined by ^{1}H NMR and ^{13}C NMR spectroscopy and further confirmed by FTIR spectroscopy. Compounds **3** and **4** were used to synthesize MPCs **3a–c** and **4a–c**. The Zn, Mg, and Co Pcs **3a–c** and **4a–c** were obtained from the corresponding metal salts, $Zn(CH_3COO)_2$, $MgCl_2$, or $CoCl_2$, in *n*-pentanol and using 1,8-diazabicyclo[5,4,0]undec-7-ene (DBU) as the catalyst. The Zn, Mg, and Co Pcs were purified by column chromatography using an alumina gel (Al_2O_3) column with chloroform–methanol as the eluent.

Solubility is an important factor for electrochemical- and metal-sensing applications and our synthesized MPcs are highly soluble in common organic solvents such as chloroform, tetrahydrofuran (THF), dimethylformamide (DMF), and dimethyl sulphoxide (DMSO). The MPcs **3a**, **3b** and **4a**, **4b** were dissolved in $CDCl_3$ to record their ^{1}H NMR spectra, while MPcs **3a**–**4c** were dissolved in THF for cyclic voltammetric measurements. MPcs **3a** and **4a** and all of the metal salts were dissolved in a mixture of acetonitrile/chloroform in a 1:1 ratio for fluorometric metal ion titrations.

Structure elucidation

Spectroscopic techniques were used to identify the structures of the phthalonitriles. In the FTIR spectra of phthalonitrile compounds **3** and **4** the disappearance of the OH groups of **1** and **2** (3380 cm^{-1}) and the presence of characteristic stretching bands for C≡N groups at 2232 and 2232 cm^{-1} were indicative of succesful coupling. No change was observed in the other bands of the spectra except for minor shifts. Other IR stretching vibrations of **3** and **4** were similar to those of compounds **1** and **2**. Additional characteristic vibration peaks were observed for **3** and **4**: aromatic C–H stretches at 3071 cm^{-1} (for **3**) and 3073 cm^{-1} (for **4**), carbonyl groups (C=O) at 1665 cm^{-1} (for **3**) and 1663 cm^{-1} (for **4**), Ar–C=C group stretches of at 1596–1578 cm^{-1} (for **3**) and 1595–1481 cm^{-1} (for **4**) and ether group (ArC–O–CAr) stretches at 1308–1247 cm^{-1} (for **3**) and 1311–1244 cm^{-1} (for **4**).

In the ^{1}H NMR spectra of the phthalonitrile compounds (Figure 1), the OH group at 12.8 ppm had disappeared and aromatic protons appeared at around 8.00–7.15 ppm. The ^{13}C NMR spectra of compounds **3** and **4** indicated the presence of nitrile carbon atoms (C≡N) at 121.80 and 121.64 (for **3**) and 117.93 and 117.72 ppm (for **4**), respectively. The observed molecular ion peaks of phthalonitrile compounds **3** and **4** are shown in Supporting Information (Table 1). Due to the difficult ionization of these compounds, we were unable to obtain a clear ion peak.

The disappearance of the C≡N vibration band at 2232 cm^{-1} is considered as evidence of the formation of zinc(II) PCs **3a** and **4a**, magnesium(II) PCs **3b** and **4b**, and cobalt(II) PCs **3c** and **4c**. The ^{1}H NMR spectra of the zinc(II) PC complexes **3a** and **4a** showed the presence of aromatic protons at 7.29 ppm (s, 52H, ArH) while magnesium(II) PC complexes **3b** and **4b** showed the aromatic protons at 7.28 ppm (s, 52H, ArH) because of aggregation. Due to the paramagnetic nature of complexes **3c** and **4c**, the ^{1}H NMR spectra of these compounds could not be determined.[28]

In the mass spectra of the zinc, magnesium, and cobalt Pcs, the presence of molecular ion peaks at *m/z* = 1844.39 $[M + Na + K]^+$ for **3a**; 1538.74 $[M]^+$ for **4a**; 1742.06 $[M + H]^+$ for **3b;** 1498.35 $[M + H]^+$ for **4b**; 1841.45 $[M + 2MeOH]^+$ for **3c**; and 1587.84 $[M + Na + MeOH]^+$ for **4c**, confirmed the proposed structures (see Supporting Information).

UV-Vis absorption spectra and aggregation properties

PC complexes in the UV-Vis region show two strong absorptions regions; the first one is at 300–500 nm and is called the B band. The second, the more energetic absorption, is known as the Q band, and occurs at near 600–700 nm.[29] The UV-Vis absorption spectra of the synthesized zinc, magnesium, and cobalt PCs **3a–c, 4a–c** in DMF at 1.2×10^{-5} M

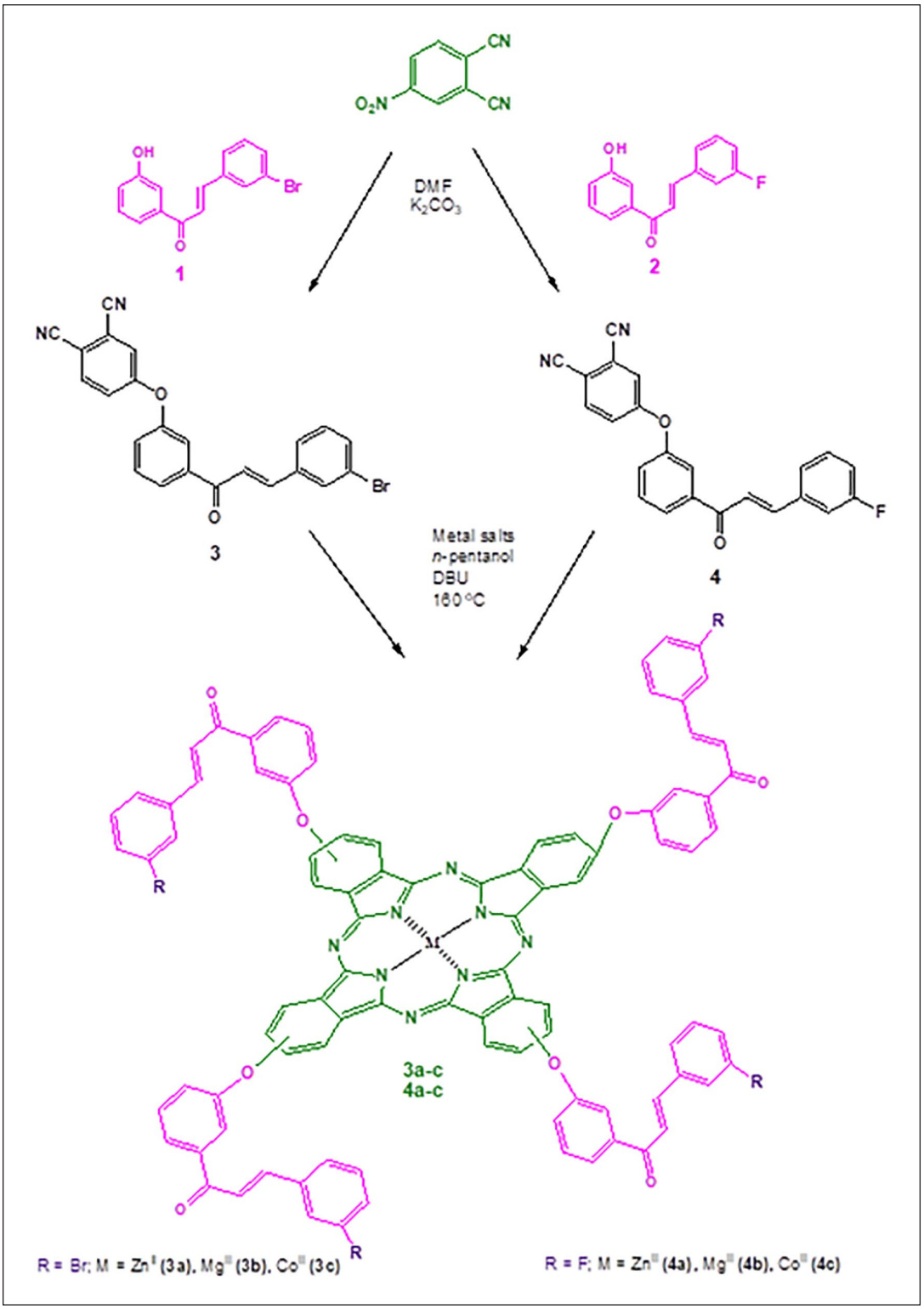

Scheme 1. The synthetic route to the metallophthalocyanines.

concentration are shown in Figures 2 and 3. The UV-Vis absorption spectra show Q band absorptions at 680/613 (corresponding to degenerate D_{4h} symmetry), 680/614, 680/613, 679/613, 667/613, and 674/613 nm, respectively, while the B band absorptions were observed at 385, 385/337, 384, 385/326, 328, and 380 nm, respectively (Table 1).

The MPCs **3a–c** have the same periphery, but they have different metal ions in the core. Their Q band positions were similar due to the same substituent on their peripheries (Figure 2). However, CoPc **3c** showed a blue-shifted Q band when compared with the other PC complexes **3a** and **3b**. The intensity of the Q bands of PC **3a–c** followed the order: ZnPc > MgPc > CoPc.

As shown in Figure 3, PC complexes **4a–c,** having the same substituent, but containing different metal atoms in the core, showed similar Q band positions in the UV-Vis spectra. The Q band intensity of PCs **4a–c** was ZnPc > MgPc > CoPc.

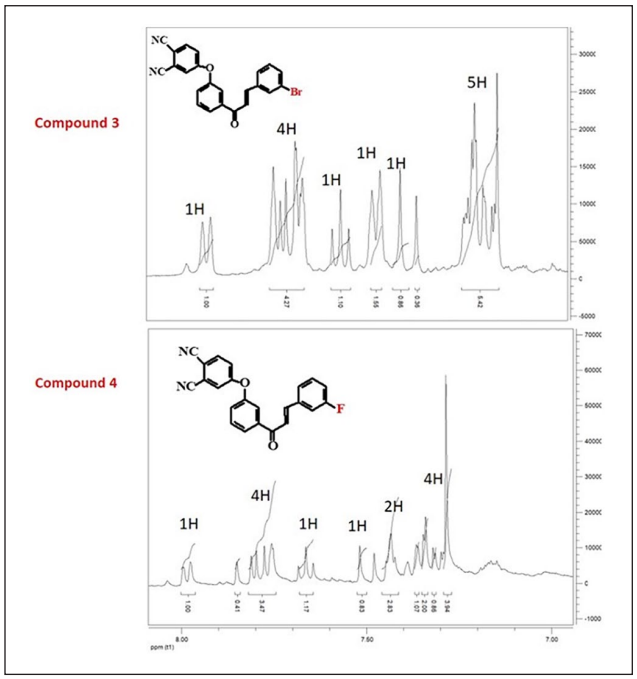

Figure 1. ^{1}H NMR spectra of phthalonitrile compounds **3** and **4**

Table 1. Absorption spectral data of novel metallophthalocyanine compounds **3a–c** and **4a–c** in DMF.

Compound	Q band λ_{max} (nm)		log ε		B band λ_{max} (nm)		log ε	
3a	680	613	4.88	4.28	385		4.46	
4a	680	614	4.58	4.03	385	337	4.23	4.51
3b	680	613	4.65	4.08	384		4.29	
4b	679	613	3.91	3.62	385	326	3.84	4.19
3c	667	613	4.34	4.04	328		4.58	
4c	674	613	4.09	3.78	380		3.92	

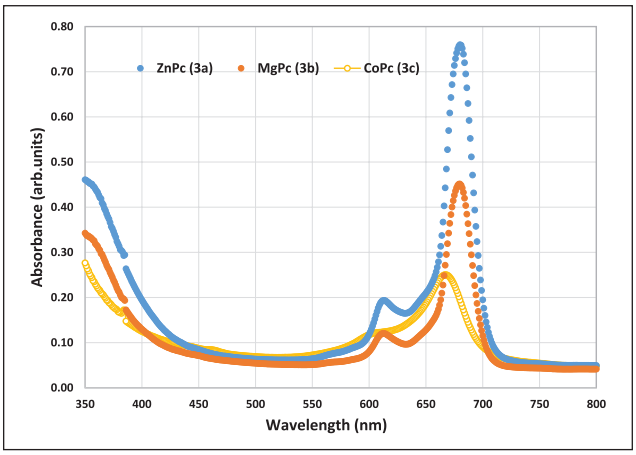

Figure 2. UV-Vis spectra of phthalocyanine compounds **3a–c** in DMF at 12×10^{-6} M concentration.

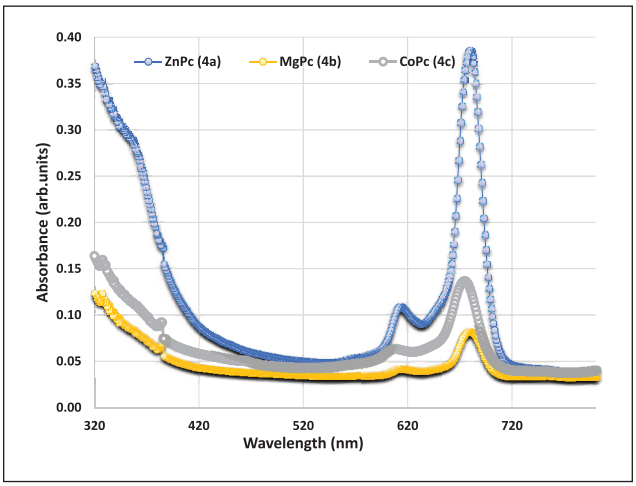

Figure 3. UV-Vis spectra of phthalocyanine compounds **4a–c** in DMF at 12×10^{-6} M concentration.

Aggregation depends on the concentration, solvent, temperature, metal ions, and structures of the substituents.[30] Aggregation of the PC compounds is generally examined by changing the concentration of the PC or by changing the solvent. These factors will affect the shape and position of the Q band when aggregation happens.

In this study, the aggregation behavior of the MPC complexes **3a–c** and **4a–c** were investigated in different solvents and changed with increased concentration according to UV-Vis spectroscopy (Figures 4 and 5). We know that the absorption intensities of Q bands are markedly changed by the solvent. The effect of different solvents on the aggregation properties of the ZnPcs **(3a, 4a)**, MgPcs **(3b, 4b)**, and CoPcs **(3c, 4c)** can be seen in Figure 4.

Compound **3a** showed the highest absorbance values in DMF and THF and the lowest absorbance value in ethanol. In addition, the position of the Q bands of compound **3a** in DMF and THF indicated a slight shift (ca. 4 nm) to higher energy in comparison with other solvents. The absorbance data shows that **3a** showed aggregation, especially in ethanol. The UV-Vis absorption spectra of **4a** in different solvents showed the highest absorbance value in THF and the lowest absorbance value in ethanol. Also, compound **4a** in the ethyl acetate, diethyl ether, and THF showed a slight shift (ca. 2–3 nm) to lower energy in comparison with the other solvents in the UV-Vis absorption spectra. The UV-Vis absorption spectra of **3b** showed the highest absorbance in DMF, while that of **4b** occured in $CHCl_3$. The lowest absorbance values of **3b** and **4b** were observed in ethanol and diethyl ether, respectively. In addition, compound **3b** in ethyl acetate and THF showed a slight shift (ca. 2 nm) to lower energy in comparison with the other solvents, while **4b** underwent a slight shift (ca. 3–4 nm) to the lower energy in ethyl acetate, DMF, THF, and diethyl ether.

The UV-Vis absorption spectra of cobalt PCs **3c** and **4c** in different solvents are also shown in Figure 4. The highest absorbance value of **3c** was observed in diethyl ether and the lowest absorbance value in acetonitrile and ethanol. The CoPc complex **3c** undergoes *H-type* aggregation in acetonitrile, $CHCl_3$, CH_2Cl_2, DMF, THF, ethanol, DMSO, and EtOAc. The UV-Vis absorption spectra of **4c** showed the highest absorbance values in DMF and diethyl ether and the lowest absorbance values in ethanol. Compound **4c** was the most aggregated in ethanol compared with the other solvents.

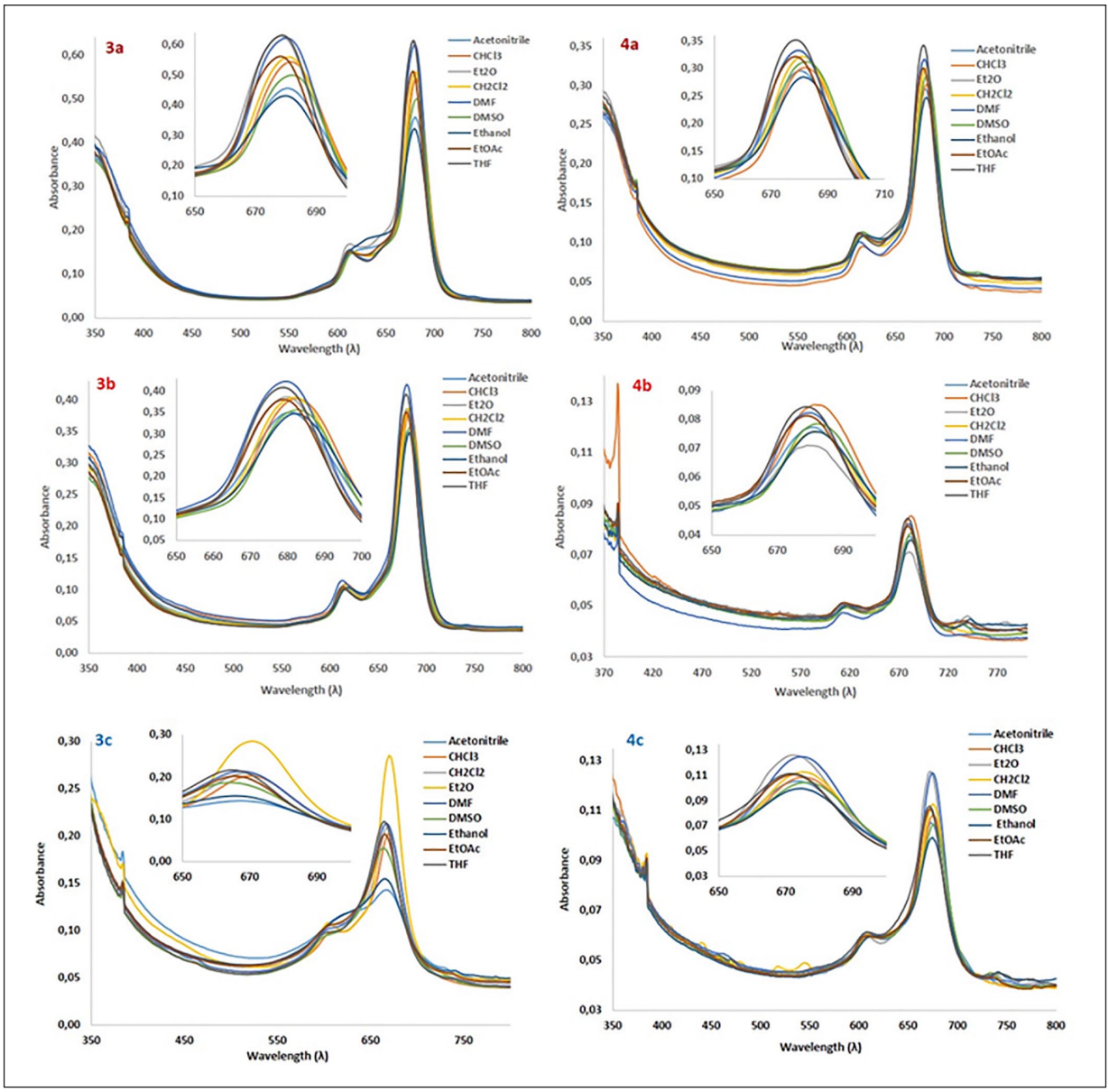

Figure 4. Absorption spectra of ZnPcs **(3a, 4a)**, MgPcs **(3b, 4b)**, and CoPcs **(3c, 4c)** in different solvents at 12×10^{-6} mol dm^{-3}.

The effect of changing the concentration on the aggregation properties of the ZnPcs (**3a** and **4a**), MgPcs (**3b** and **4b**), and CoPcs (**3c** and **4c**) can be seen in Figure 5. All of the studied MPCs did not aggregate in DMF at concentrations between 2×10^{-6} and 1.2×10^{-5} mol L^{-1} and they all exhibited monomeric behavior. At concentrations between 2×10^{-6} and 1.2×10^{-5} mol L^{-1}, the MPC compounds **3a–c** and **4a–c** were found to be compatible with the Beer–Lambert law.

Cyclic voltammetric measurements

The cyclic voltammetric measurements of all the MPCs were recorded on a Parstat 2273 potentiostat/galvanostat. In three-electrode systems, a Pt working electrode, a Pt counter electrode and a glassy carbon electrode, as reference, were used. As the electrolyte pure 0.1 M tetra-*n*-butylammonium tetrafluoroborate (TBAB) was used together with pure THF. Figures 6–8 show the cyclic voltammograms of the MPCs. The cyclic voltammetric measurements showed one irrevesible oxidation at about 1.0 V for the bromo-derived PC compounds **3a–c**. The cyclic voltammetric measurements also showed one irrevesible reduction at about −1.7 V for the fluoro-derived PC compounds **4a–c**. Thus, bromo and fluoro substitution gave different redox behavior to the MPCs.

Compounds **3a**, **3b** have the same half-wave potantials, $E_{1/2} = 0.92$ V. Likewise **4a**, **4b** have the same half-wave potentials, $E_{1/2} = 1.76$ V. When the central metal ion is Zn(II) or Mg(II), the bromo and fluoro substituents on the periphery of the PC ligand do not influence strongly the solution redox chemistry of these materials. When looking at compounds **3c** and **4c**, different half-wave potentials are observed. The half-wave potential of compound **3c** is 1.1 V, while the half-wave potential of compound **4c** is −1.55 V. Since cobalt(II) ions have *d* orbitals which interact electronically with the PC ring, unlike zinc and magnesium ions, the $E_{1/2}$ values of cobalt(II) PC complexes **3c** and **4c** are different. This observation is

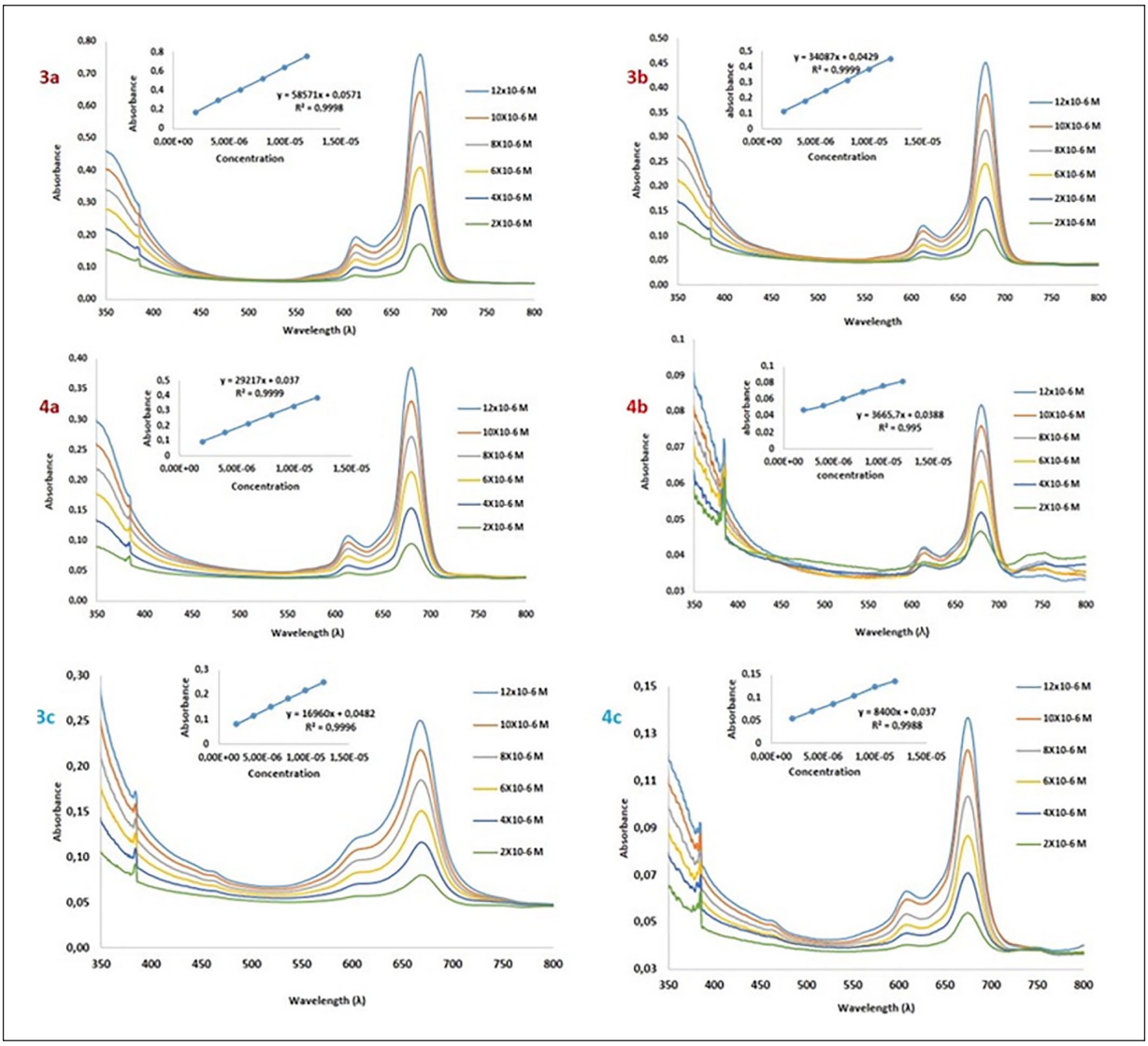

Figure 5. Absorption spectra of ZnPcs **(3a, 4a)**, MgPcs **(3b, 4b)**, and CoPcs **(3c, 4c)** in DMF at different concentrations: A; 2×10^{-6}, B; 4×10^{-6}, C; 6×10^{-6}, D; 8×10^{-6}, E; 10×10^{-6}, F; 12×10^{-6} mol dm^{-3}.

consistent with the literature in which zinc and magnesium are redox inactive and cobalt is redox active.[1,4,8]

Fluorometric metal ion titrations of Zn PC compounds **3a** *and* **4a**

The fluorescence spectra were recorded on a Hitachi F-7000 fluorescence spectrophotometer. The PC compounds **3a** and **4a** were used for titration of the metal ions, and concentrations of 6.73×10^{-5} and 1.56×10^{-4} M were used, respectively. $FeCl_3 \cdot 6H_2O$ (7.40×10^{-4} M), $3CdSO_4 \cdot 8H_2O$ (1.25×10^{-3} M), $HgCl_2$ (1.18×10^{-3} M), $CuSO_4 \cdot 5H_2O$ (8.01×10^{-4} M), $NiCl_2 \cdot 6H_2O$ (1.35×10^{-3} M), and $Co(CH_3COO)_2 \cdot 4H_2O$ (1.28×10^{-3} M) salts were used as the metal ions. All the metal salts were dissolved in a mixture of acetonitrile/chloroform in a 1:1 ratio. The PC s were also dissolved in the same solvent mixture.

The fluorescence excitation wavelength of the PC s was determined as 610 nm, and this value was used to record fluorescence spectra of the PC s. The PC s and metal ions were mixed in a 1:1 ratio and the fluorescence spectra were measured. After recording the spectra of the mixtures, the same volume of metal ion solution was added and the fluorescence spectra recorded. Thus, increased spectrum

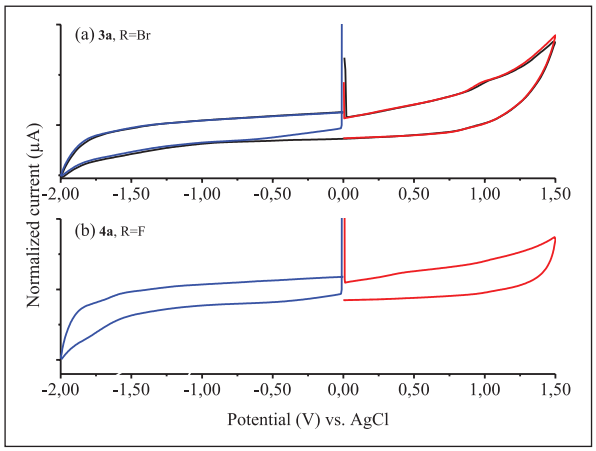

Figure 6. Cyclic voltammograms of zinc phthalocyanines **3a** and **4a**.

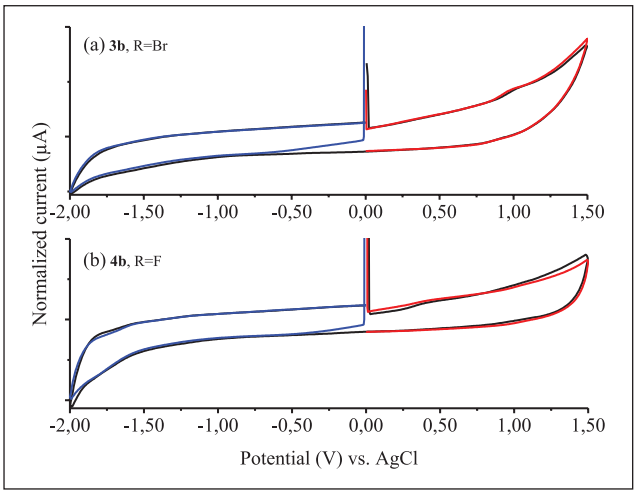

Figure 7. Cyclic voltammograms of magnesium phthalocyanines **3b** and **4b**.

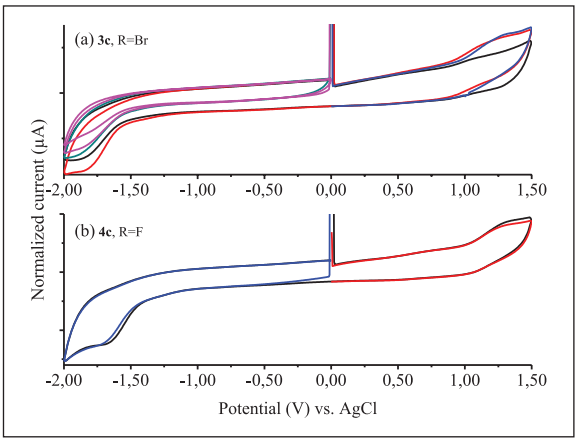

Figure 8. Cyclic voltammograms of cobalt phthalocyanines **3c** and **4c**.

intensity was recorded. The addition of the metal ion solution was repeated 10 times.

The PC compound **3a** showed no reaction versus Fe^{3+}, Hg^{2+}, and Ni^{2+} ions (Figure 9). However, Co^{2+}, Cu^{2+}, and Cd^{2+} metal ions increased the fluorescence emission intensity of compound **3a** (Figure 10). The PC compound **4a** showed a reaction versus only Cd^{2+} metal ions (Figure 10). Only Cd^{2+} metal ions increased the emission intensity of compound **4a**.

According to results of the fluroescence metal ion titrations of PC s **3a** and **4a,** it can be surmised that the bromo- and fluoro-chalcone-derived PC s show different responses to different metal ions. Thus, these results show that these halogen-substituted PC s can be used as selective sensors for different metal ions.

Conclusion

In conclusion, we have synthesized and characterized novel Zn(II), Mg(II), and Co(II) PC s which are substituted with chalcones bearing bromo or fluoro atoms. The structures of the synthesized compounds have been fully characterized by FTIR, ^{1}H NMR, ^{13}C NMR, MALDI-TOF MS, LC-HRMS, UV-Vis, and elemental analysis.

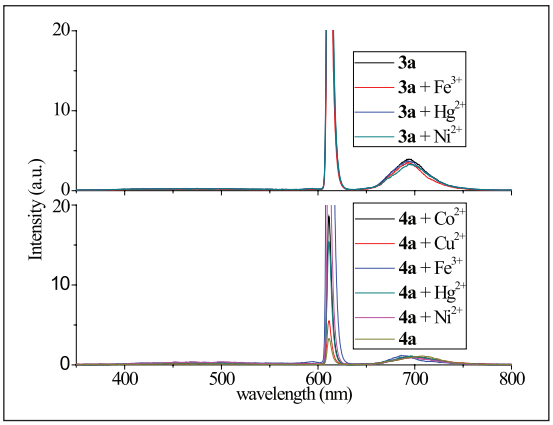

Figure 9. The metal ions that do not affect the fluorometric intensities of phthalocyanines **3a** and **4a.**

The electronic absorption spectra showed that all the MPcs were non-aggreging and were also well soluble in common organic solvents and compatible with the Beer–Lambert law. The electrochemical behavior was also investigated and the cyclic voltammograms gave one oxidation reaction for all the bromo-derived MPcs and one reduction reaction for all the fluoro-derived MPcs. Fe^{3+}, Cd^{2+}, Hg^{2+}, Cu^{2+}, Ni^{2+}, and Co^{2+} ions were titrated fluorometrically with the PC compounds **3a** and **4a,** with the bromo- and fluoro-substituted PC s showing different behavior. The bromo-substituted PC **3a** was affected by Co^{2+}, Cu^{2+}, and Cd^{2+} ions, while the fluoro-substituted PC **4a** only responded to Cd^{2+} ions. These results show that different halogen-substituted PC s can be used in metal ion titrations as selective sensors for different metal ions.

Experimental

Materials and equipment

The used materials, equipment, and spectra (IR, NMR, and mass) are supplied as supplementary information that is available online.

Synthesis

General procedure for the synthesis of phthalonitrile derivatives **3** *and* **4**. The chalcone-bound phthalonitriles were synthesized in dry DMF at 60°C by adding K_2CO_3. Equivalent amounts (1:1) of (4-nitrophthalonitrile and chalcone compounds **1** and **2** were used. The contents of the reaction vessel were stirred under a nitrogen atmosphere for 4 days. On completion of the reaction, the mixture was poured into ice-water and stirred to yield a crude product. The mixture was then filtered and dried for 3 h. The obtained crude product was purified by column chromatography using chloroform/methanol as the eluent. The reaction pathway is shown in Scheme 1.

4-{3-((2E)-3-(3-bromophenyl)prop-2-enoyl)phenoxy} phthalonitrile **(3)**. Yield: (0.59 g) 60%, m.p. 76–79°C. IR (ATR), ν_{max}/cm^{-1} = 3071 (ArH), 2232 (C≡N), 1665 (C=O), 1596–1578 (Ar–C=C), 1308–1247 (Ar–O–Ar), 751. ^{1}H NMR (400 MHz, $CDCl_3$): δ 8.00–7.98 (d, J = 8 Hz,

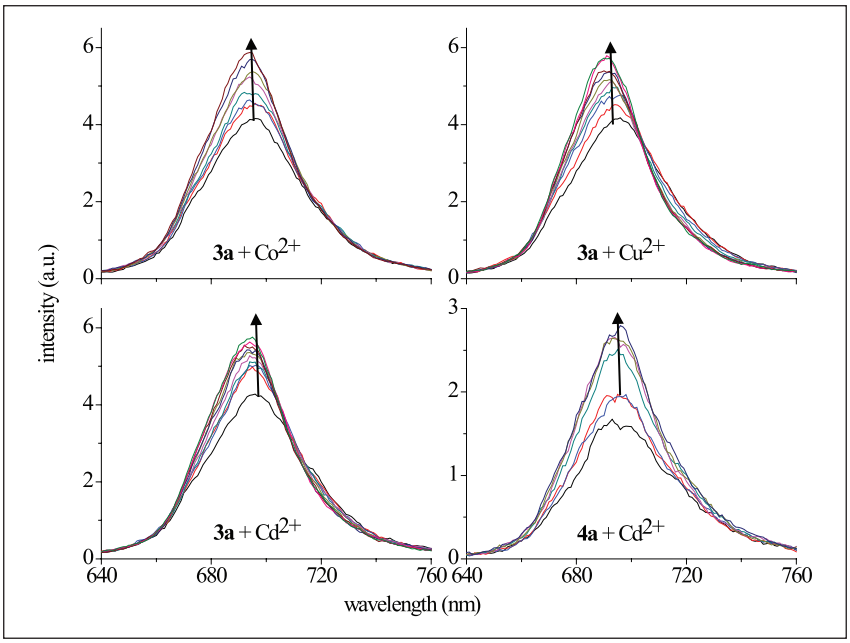

Figure 10. The metal ions that affect the fluorometric intensities of phthalocyanines **3a** and **4a.**

1H, =C–H), 7.82–7.75 (m, 4H, ArH), 7.68–7.64 (t, J = 8 Hz, 1H, ArH), 7.58–7.57 (d, J = 8 Hz, 1H, =C–H), 7.52 (s, 1H, ArH), 7.35–7.28 (m, 5H, ArH). ^{13}C NMR (400 MHz, $CDCl_3$): δ 188.42 (–C=O), 161.22, 154.21, 144.14, 140.57, 136.62, 135.58, 133.68, 131.10, 130.89, 130.58, 127.48, 126.16, 125.02, 123.19, 122.37 (ArC–Br), 121.80, 121.64, 120.42, 117.91, 115.21 (–C≡N), 114.81 (–C≡N), 109.55. MALDI-TOF-MS: m/z = 429.22 $[M]^+$. Anal. Calcd for $C_{23}H_{13}N_2O_2Br$: C, 64.35; H, 3.05; N, 6.53; found: C, 65.36; H, 3.35; N, 6.79%.

4-{3-((2E)-3-(3-fluorophenyl)prop-2-enoyl)phenoxy}phthalonitrile **(4)**. Yield: (0.46 g) 60%, m.p. 98–101°C. IR (ATR), ν_{max}/cm^{-1} = 3073 (ArH), 2232 (C≡N), 1663 (C=O), 1595–1481 (Ar–C=C), 1311–1244 (Ar–O–Ar), 782. ^{1}H NMR (400 MHz, $CDCl_3$): δ 7.99 (d, J = 8 Hz, 1H, =C–H), 7.81–7.75 (d, J = 9 Hz, 1H, ArH), 7.68–7.64 (t, J = 8 Hz, 1H, ArH), 7.51 (s, 1H, ArH), 7.44–7.42 (m, 2H, =C–H and ArH), 7.36–7.28 (m, 4H, ArH). ^{13}C NMR (400 MHz, $CDCl_3$): δ 188.15 (C=O), 164.30 (d, $^1J_{C\text{-}F}$ = 246.5 Hz), 161.21, 154.22, 144.49, 144.47, 140.62, 136.80, 136.72, 135.57, 131.09, 130.69 (d, $^3J_{C\text{-}F}$ = 8 Hz), 126.13, 124.97, 124.77 (d, $^4J_{C\text{-}F}$ = 2.7 Hz) 121.79, 121.63, 120.40, 117.93 (d, $^2J_{C\text{-}F}$ = 20.8 Hz), 115.19 (–C≡N), 114.79 (d, $^2J_{C\text{-}F}$ = 11.9 Hz), 114.45 (–C≡N), 109.57. MALDI-TOF-MS: m/z = 368.35 $[M]^+$. Anal. Calcd for $C_{23}H_{13}N_2O_2F$: C, 74.99; H, 3.56; N, 7.60; found: C, 75.05; H, 3.94; N, 7.35%.

General procedure for the synthesis of MPCs **3a, 4a; 3b, 4b; and 3c, 4c**. The chalcone-substituted phthalonitriles, **3** or **4** (0.44 mmol) and the anhydrous metal salt ($Zn(CH_3COO)_2$, $MgCl_2$, or $CoCl_2$ (0.11 mmol)) were dissolved in *n*-pentanol (2 mL) and DBU (6 drops). Next, the mixture was stirred at reflux under a nitrogen atmosphere at 160°C for 24 h. The reaction mixture was poured into ethanol. The obtained green precipitate was filtered and washed with hot ethanol and methanol. The synthesized metallophthalocyanine complexes were purified on an alumina gel (Al_2O_3) column with chloroform–methanol (10:4) for compound **3a;** (10:2) for compound **4a;** (10:1) for compound **3b;** (10:2) for compound **4b;** (10:4) for compound **3c;** and (10:3) for compound **4c** as eluent (Scheme 1).

The spectral data of MPCs **3a, 4a; 3b, 4b; and 3c, 4c**. **3a (ZnPc)**: Yield: (23.5 mg) 12%, m.p. >300°C. IR (ATR), ν_{max}/cm^{-1} = 3066 (ArH), 1719 (C=O), 1578–1437 (Ar–C=C), 1243 (Ar–O–Ar), 783. ^{1}H NMR (400 MHz, $CDCl_3$): δ 7.29 (s, 52H, ArH). MALDI-TOF-MS: m/z = 1844.39 $[M + Na + K]^+$. UV-Vis (DMF): λ_{max}, nm (log ε) = 680 (4.81), 618 (4.23), 342 (4.62). Anal. Calcd for $C_{92}H_{52}N_8O_8Br_4Zn$: C, 61.94; H, 2.92; N, 6.28; found: C, 61.42; H, 2.50; N, 5.96%.

4a (ZnPc): Yield: (20 mg) 12%, m.p. >300°C. IR (ATR), ν_{max}/cm^{-1} = 3066 (ArH), 1717 (C=O), 1648–1578 (Ar–C=C), 1259–1225 (Ar–O–Ar), 784. ^{1}H NMR (400 MHz, $CDCl_3$): δ 7.29 (s, 52H, ArH). MALDI-TOF-MS: m/z = 1538.74 $[M]^+$. UV-Vis (DMF): λ_{max}, nm (log ε)= 680 (4.52), 613 (3.99), 384 (4.20). Anal. Calcd for $C_{92}H_{52}N_8O_8F_4Zn$: C, 71.74; H, 3.38; N, 7.28; found: C, 71.57; H, 3.56; N, 7.55%.

3b (MgPc): Yield: (28.7 mg) 15%, m.p. >300°C. IR (ATR), ν_{max} /cm^{-1} = 3066 (ArH), 1718 (C=O), 1578–1475 (Ar–C=C), 1243 (Ar–O–Ar), 784. ^{1}H NMR (400 MHz, $CDCl_3$): δ 7.28 (s, 52H, ArH). MALDI-TOF-MS: m/z = 1742.06 $[M + H]^+$. UV-Vis (DMF): λ_{max}, nm (log ε) = 680 (4.59), 613 (4.04), 325 (4.55). Anal. Calcd for $C_{92}H_{52}N_8O_8Br_4Mg$: C, 63.39; H, 2.98; N, 6.43; found: C, 63.86; H, 2.71; N, 6.95%.

4b (MgPc): Yield: (24.7 mg) 15%, m.p. >300°C. IR (ATR), ν_{max}/cm^{-1} = 3070 (ArH), 1717 (C=O), 1567–1438 (Ar–C=C), 1259–1226 (Ar–O–Ar), 785. ^{1}H NMR ($CDCl_3$): δ 7.28 (s, 52H, ArH). MALDI-TOF-MS: m/z = 1498.35

$[M + H]^+$. UV-Vis (DMF): λ_{max}, nm (log ε): 679 (3.88), 615 (3.61), 380 (3.78). Anal. Calcd for $C_{92}H_{52}N_8O_8F_4Mg$: C, 73.71; H, 3.47; N, 7.47; found: C, 73.69; H, 3.64; N, 7.51%.

3c (CoPc): Yield: (27.4 mg) 14%, m.p. >300°C. IR (ATR), ν_{max}/cm^{-1} = 3064 (ArH), 1716 (C=O), 1645–1435 (Ar–C=C), 1322, 1240 (Ar–O–Ar), 784. MALDI-TOF-MS: *m/z* = 1841.45 $[M + 2MeOH]^+$. UV-Vis (DMF): λ_{max}, nm (log ε) = 667 (4.34), 613 (4.04), 328 (4.58). Anal. Calcd for $C_{92}H_{52}N_8O_8Br_4Co$: C, 62.16; H, 2.93; N, 6.31; found: C, 62.44; H, 2.73; N, 6.02%.

4c (CoPc): Yield: (23.6 mg) 14%. m.p. >300°C. IR (ATR) ν_{max}/cm^{-1} = 3064 (ArH), 1716 (C=O), 1645–1437 (Ar–C=C), 1243 (Ar–O–Ar), 783. MALDI-TOF-MS: *m/z* = 1587.84 $[M + Na + MeOH]^+$. UV-Vis (DMF): λ_{max}, nm (log ε) = 674 (4.09), 610 (3.78), 380 (3.92). Anal. Calcd for $C_{92}H_{52}N_8O_8F_4Co$: C, 72.05; H, 3.39; N, 7.31; found: C, 72.21; H, 3.59; N, 7.64%.

Declaration of conflicting interests

The author(s) declared no potential conflicts of interest with respect to the research, authorship, and/or publication of this article.

Funding

The author(s) disclosed receipt of the following financial support for the research, authorship, and/or publication of this article: This study was supported by the Research Fund of Artvin Çoruh University, Project no: 2018.F91.02.01 (Artvin-Turkey). Huseyin Karaca is grateful to the research fund of Sakarya University (BAPK: 2018-3-12-165).

ORCID iDs

Ayse Aktas Kamiloglu https://orcid.org/0000-0002-7347-4018
Gonca Celik https://orcid.org/0000-0002-4634-3354

Supplemental material

Supplemental material for this article is available online.

References

1. Leznoff CC and Lever ABP. *Phthalocyanines, properties and applications*, vols. 1–4. New York: VCH, 1989–1996.
2. Hanack M, Schneider T, Barthel M, et al. *Coord Chem Rev* 2001; 219–221: 235–258.
3. Jeong J, Kumar RS, Mergu N, et al. *J Mol Struct* 2017; 1147: 469–479.
4. Karaca H. *J Organomet Chem* 2016; 822: 39–45.
5. Vashurin A, Maizlish V, Tikhomirova T, et al. *J Mol Struct* 2018; 1160: 440–446.
6. Riquelme J, Neira K, Marco JF, et al. *Electrochim Acta* 2018; 265: 547–555.
7. Suzuki A, Okumura H, Yamasaki Y, et al. *App Surface Sci* 2019; 488: 586–592.
8. Koca A, Kalkan A and Bayır ZA. *Electrochim Acta* 2011; 56: 5513–5525.
9. Palacin S. *Adv Colloid Interface Sci* 2000: 87; 165–181.
10. Sen P, Managa M and Nyokong T. *Inorg Chim Acta* 2019; 491: 1–8.
11. Banasz R and Wałęsa-Chora M. *Coord Chemiy Rev* 2019; 389: 1–18.
12. Erbahar DD, Harbeck M, Gümüş G, et al. *Sens Actuators B Chem* 2014; 190: 651–656.
13. Klyamer DD, Basova TV, Krasnov PO, et al. *J Mol Struct* 2019; 1189: 73–80.
14. Aktas Kamiloglu A, Acar I and Biyiklioglu. Z *Polyhedron* 2017; 137:10–16.
15. Karaca H, Sezer S, Ozalp-Yaman S, et al. *Polyhedron* 2014; 72: 147–156.
16. Bagdassarian VLC, Bagdassarian KS and Atanassova MS. *Mintage J Pharm Med Sci* 2013; 2: 26–31.
17. Go ML, Wu X and Liu XL. *Curr Med Chem* 2005; 12: 481–99.
18. Bhat BA, Dhar KL, Puri SC, et al. *Bioorg Med Chem Lett* 2005; 15: 3177–3180.
19. Jurasek A, Knoppava V, Dandarova M, et al. *Tetrahedron* 1978; 34: 1833–1836.
20. Motta LF, Gaudio AC and Takahata Y. *Internet Electron J Mol Des* 2006; 5: 555–569.
21. Karaca H, Cayeğil B and Sezer S. *Synth Met* 2016; 215: 134–141.
22. Zhao J, Qiu J, Gou X, et al. *Chin J Catal* 2016; 37: 571–578.
23. Shalini S, Balasundara Prabhu R, Prasanna S, et al. *Renew Sustain Energy Rev* 2015; 51: 1306–1325.
24. Herndon JW. *Coor Chem Rev* 2018; 377: 86–190.
25. Syam S, Abdelwahab SI, Al-Mamary MA, et al. *Molecules* 2012; 17: 6179–6195.
26. Kaur N and Kumar S. *Tetrahedron* 2011; 67: 9233–9264.
27. Khazaal MB, Al-hambani AM and A-Faeq A. *Mintage J Pharm Med Sci* 2016; 5: 24–32.
28. Aktas Kamiloglu A, Aydemir M, Acar I, et al. *Karadeniz Chem Sci Tech* 2017; 1: 22–30.
29. Demirbaş Ü, Akyüz D, Akcay HT, et al. *J Mol Struct* 2019; 1176: 695–702.
30. Kantekin H, Yalazan H, Kahriman N, et al. *J Photochem Photobiol A Chem* 2018; 361: 1–11.